

# Topogivity: A Machine-Learned Chemical Rule for Discovering Topological Materials

Andrew Ma,<sup>1,\*</sup> Yang Zhang,<sup>2,\*</sup> Thomas Christensen,<sup>2</sup> Hoi Chun Po,<sup>2,3</sup> Li Jing,<sup>2,4</sup> Liang Fu,<sup>2,†</sup> and Marin Soljačić<sup>2,‡</sup>

<sup>1</sup>Department of Electrical Engineering and Computer Science, Massachusetts Institute of Technology, Cambridge, Massachusetts 02139, USA

<sup>2</sup>Department of Physics, Massachusetts Institute of Technology, Cambridge, Massachusetts 02139, USA

<sup>3</sup>Department of Physics, Hong Kong University of Science and Technology, Clear Water Bay, Hong Kong, China

<sup>4</sup>Facebook AI Research, New York, New York 10003, USA

Topological materials present unconventional electronic properties that make them attractive for both basic science and next-generation technological applications. The majority of currently-known topological materials have been discovered using methods that involve symmetry-based analysis of the quantum wavefunction. Here we use machine learning to develop a simple-to-use heuristic chemical rule that diagnoses with a high accuracy whether a material is topological using only its chemical formula. This heuristic rule is based on a notion that we term *topogivity*, a machine-learned numerical value for each element that loosely captures its tendency to form topological materials. We next implement a high-throughput strategy for discovering topological materials based on the heuristic topogivity-rule prediction followed by ab initio validation. This way, we discover new topological materials that are not diagnosable using symmetry indicators, including several that may be promising for experimental observation.

Topological materials – including both topological insulators [1–5] and topological semimetals [6–9] – are unconventional phases of matter characterized by topologically nontrivial electron wavefunctions. Since the beginning of the field, an important and enduring question has been how to determine if a given electronic material is topological. Efforts to answer this question have largely relied on first-principles calculations in synergy with topological band theory [10, 11]. In particular, recently-developed theories known as symmetry indicators [12] and topological quantum chemistry [13] enable the diagnosis of a wide range of topological materials using symmetry-based analysis of the wavefunction [14–16]. These symmetry-based methods require relatively low computational cost and have enabled high-throughput computational searches for topological materials [17–19].

Despite these successes, symmetry indicators do not apply to materials having low symmetry crystal structures [12], and therefore cannot diagnose all topological materials. For example, the first experimentally-observed Weyl semimetal, tantalum arsenide (TaAs) [7, 20], is a non-symmetry-diagnosable topological material [17]. Its topological nature is established by calculating wavefunction-based topological invariant directly [21], which involves significant computational cost. From a broad conceptual standpoint, topological materials such as Chern insulators and time-reversal-invariant  $Z_2$  topological insulators are robust against any small perturbation breaking all crystal symmetries, which renders symmetry indicators inapplicable even though topology remains intact. Thus, for both practical and fundamental reasons, it is highly desirable to develop accurate and simple-to-use rules to determine whether *any* given material is topological.

Many aspects of quantum solids can be understood at a heuristic level from a chemistry perspective. A well-known example is bonding, which can be understood using quantum-mechanical approaches such as molecular orbital theory [22],

as well as using heuristics such as the difference of element electronegativities. While quantum theory can provide greater detail and accuracy, chemical heuristics can often provide valuable insight and a useful guide for materials discovery. Is there a deep chemical reason why a particular material is topological? To what extent can topological materials be understood and identified using chemical heuristic approaches? While connections between chemistry and electronic band topology (e.g., based on the presence or absence of certain elements) have been explored [23–27], existing chemical heuristics do not provide a broadly applicable path for finding topological materials.

Here, we use machine learning (ML) to help us search for chemical origins of topological electronic structure in materials. Recently, ML has become a powerful approach for advancing scientific discovery in materials science [28–30]. In the area of topological materials, researchers have begun to apply ML to both toy models [31–34] and ab initio data [35–40]. While ML has led to important advances for many applications in engineering and science, most ML models act essentially like black boxes: they are complicated models which often provide correct answers, but because of their complexity, they are difficult to understand, and hence provide little insight and intuition about the systems they are applied to. Since a key aim of our work is precisely to learn insights about topology, we instead focus our quest onto interpretable ML models, with a goal of finding a broadly applicable heuristic chemical rule that diagnoses whether or not a material is topological.

The heuristic rule that our ML approach discovered is based on the notion of a learned parameter for each element that loosely captures the tendency of an element to form topological materials. We refer to this as an element’s *topogivity*. This heuristic rule is simple, hand-calculable, and interpretable: a given material is diagnosed with high accuracy (typically > 80%) as topologically nontrivial (trivial) if the weighted average of its elements’ topogivities is positive (negative) (Fig. 1a). The heuristic rule does not rely on crystal symmetry and our approach can be used to make predictions on *all* materials. We integrate the heuristic rule into a high-throughput procedure to search for non-symmetry-diagnosable

\* A.M. and Y.Z. contributed equally to this work.

† liangfu@mit.edu

‡ soljagic@mit.edu

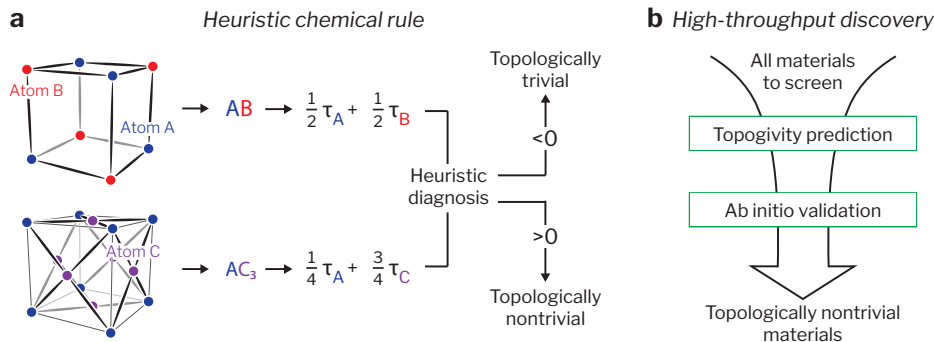


**Figure 1. Topogivity-based diagnosis and discovery of topological materials.** **a** Given a stoichiometric material, the topogivity-based heuristic diagnosis is evaluated by simply weighting the material’s elements’ (A, B, and C) topogivities ( $\tau_A$ ,  $\tau_B$ , and  $\tau_C$ ) by their relative abundance in the chemical formula ( $AB$  and  $AC_3$ ). The sign indicates the topological classification and the magnitude indicates roughly how confident we are in this classification. Each element’s topogivity is a machine-learned parameter that loosely captures the element’s tendency to form topologically nontrivial materials. **b** We leverage our framework to perform high-throughput topological materials discovery. First, we use the topogivities to rapidly screen through a suitable collection of materials (i.e. the discovery space) in order to find candidate topological materials. Subsequently, we carry out ab initio validation by performing DFT on these candidates. We discovered topological materials that are not diagnosable using the standard symmetry indicators approach [12].

topological materials, in which we perform screening using the heuristic rule followed by density functional theory (DFT) validation (Fig. 1b). The newly-discovered topological materials include several high-quality examples that may be promising for experimental realization.

## CLASSES OF MATERIALS

Conventional textbook chemistry teaches that the electrons of insulators (including semiconductors) are localized to ionic or covalent bonds, while the electrons of metals are delocalized and “free”. From a band-theoretic perspective, the former make up part of the class of materials known as atomic insulators and the latter roughly correspond to “ordinary” metals. Topological insulators and topological semimetals do not fit into this conventional dichotomy. Topological insulators feature a band gap and a nontrivial topological invariant, and as a consequence, their electronic states cannot be reduced to an assembly of localized atomic or molecular orbitals. Topological semimetals have band degeneracies protected by symmetry or topology near or at the Fermi level. Collectively, we refer to topological insulators and topological semimetals as topological materials, and refer to all other materials as trivial materials.

To learn a heuristic chemical rule for diagnosing topological materials, we employ a supervised learning approach. This requires a labeled dataset in which each material is labeled as “topological” or “trivial”. The learned heuristic chemical rule is then applied to screen another dataset which we refer to as the discovery space. Existing ab initio databases of stoichiometric, non-magnetic, three-dimensional materials [17–19, 41] offer a convenient source of data. However, it is important to note that they are imperfect, in part because the symmetry-based high-throughput screening methods that were used to generate them are inherently incapable of detecting certain topology. Taking such limitations into account, we identify the labeled

dataset as a subset of the database generated by Tang *et al.* [17] (see Supplementary Section S1) (our methodology could also be applied to other databases that contain both trivial materials and topological materials). Our labeled dataset consists of 9,026 materials, of which 51% are labeled as trivial and the remaining 49% are labeled as topological. However, due to the aforementioned imperfection, for ML purposes this labeled dataset should effectively be considered as a dataset with noisy labels, e.g., some topological materials are incorrectly labeled as trivial. Separately, the discovery space consists of 1,433 materials, whose topology cannot be determined from the symmetry indicators method (see Supplementary Section S1). By applying the learned heuristic chemical rule to the discovery space and then performing DFT, we are able to evaluate its ability to predict topological materials beyond those diagnosable by existing standard approaches. Some of the topological materials that we identify in the discovery space are known elsewhere in the literature and serve primarily as confirmations, whereas others represent instances of truly new materials discovery.

## LEARNING A HEURISTIC CHEMICAL RULE

Our machine learning model takes the form of a heuristic chemical rule. Specifically, the model maps each material  $M$  to a number  $g(M)$  according to the function

$$g(M) = \sum_E f_E(M)\tau_E,$$

where the summation runs over the elements present in the chemical formula of material  $M$ ,  $\tau_E$  is a learned parameter for each element  $E$ , and  $f_E(M)$  is the element fraction for the element  $E$  in material  $M$  (e.g., for a chemical formula  $A_xB_yC_z$ ,  $f_A(M) = \frac{x}{x+y+z}$ ,  $f_B(M) = \frac{y}{x+y+z}$ , and  $f_C(M) = \frac{z}{x+y+z}$ ). Classification decisions are made according to the sign of  $g(M)$ : classify as topological if positive and classify as trivial if

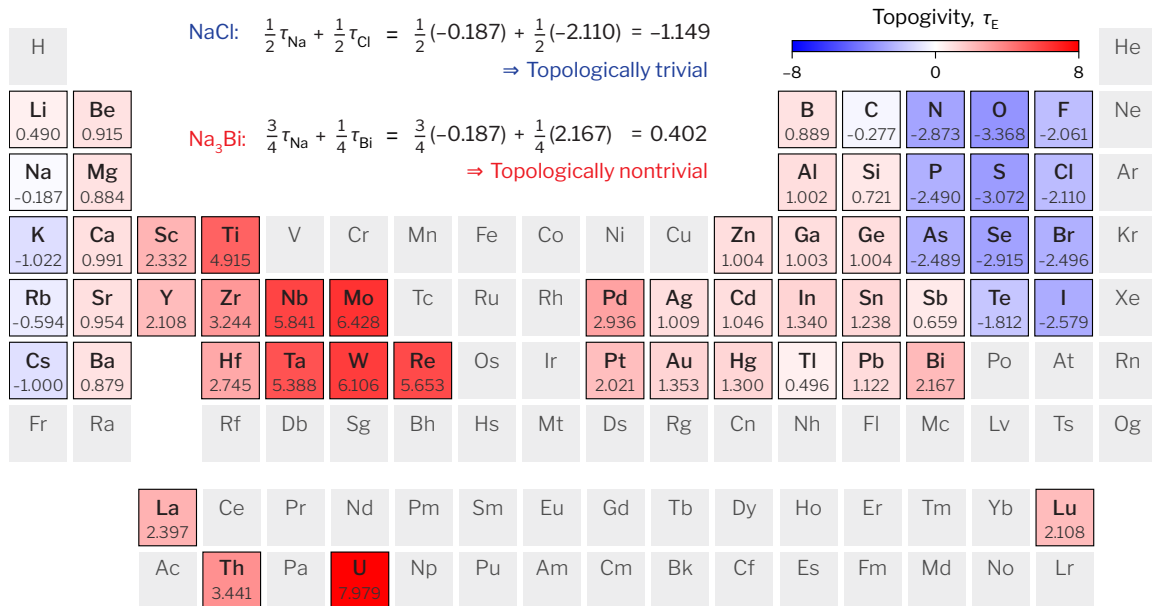


**Figure 2. Periodic table of topogivities.** Machine-learned topogivities  $\tau_E$  are shown by color-coding and in values. Elements that do not appear in any material in the dataset are shown in gray. Example applications of the topogivity-based heuristic chemical rule are shown for two materials, NaCl (trivial) and Na<sub>3</sub>Bi (nontrivial) [6].

negative. A greater magnitude of  $g(M)$  roughly corresponds to a more confident classification decision. We refer to the model as a heuristic *chemical* rule in the sense that all the information required for obtaining a diagnosis is contained in the material’s chemical formula. Additional modeling and methodological details are provided in Supplementary Sections S2.A and S2.B.

For each element  $E$ , we refer to the optimized parameter  $\tau_E$  as its *topogivity*. For a given material  $M$ ,  $g(M)$  is simply the weighted average of its elements’ topogivities, where the weighting is with respect to each element’s relative abundance, as identifiable from the material’s chemical formula. Conceptually, an element’s topogivity loosely captures its tendency to form topological materials – greater topogivity is intended to roughly correspond to a greater tendency (see Supplementary Section S2.F for details and caveats on the meaning of topogivity).

Before making predictions in the discovery space, we want to first evaluate model performance within the labeled dataset. To do this, we use a nested cross validation procedure and average the results over multiple test sets. We find an average of 82.7% accuracy. Additionally, we find empirical evidence that as the magnitude of  $g(M)$  is increased, the fraction of correctly-classified materials first increases and then plateaus, with the plateau beginning around  $|g(M)| \approx 1$ . We heuristically set a threshold of 1.0 for a high-confidence topologically nontrivial classification and observe on average that 93.0% of materials with  $g(M) \geq 1.0$  are correctly classified. After we are done doing nested cross validation, we then proceed to use the entire labeled dataset to fit the final model, which is what we will use for making predictions in the discovery space. Details and extended results are presented in Supplementary Sections S2.C, S2.D, and S2.E.

We visualize the final model’s learned topogivities in Fig. 2.

This periodic table of topogivities enables an immediate heuristic diagnosis of any stoichiometric material whose elements are featured in the table. This is illustrated with examples in Fig. 2 for the trivial insulator NaCl and the Dirac semimetal Na<sub>3</sub>Bi [6]. The Weyl semimetal TaAs [7] is also worth highlighting: TaAs is non-symmetry-diagnosable [17] and does not appear in the labeled dataset, but is successfully diagnosed as topological by the topogivity approach:  $g(\text{TaAs}) = \frac{1}{2}\tau_{\text{Ta}} + \frac{1}{2}\tau_{\text{As}} = 1.450$ .

The simplicity of our model enables us to readily extract chemical insights from the periodic table of topogivities. First, we observe that elements that are near each other in the periodic table tend to have similar topogivities, which is consistent with intuition. Second, we observe that the elements with negative topogivities are located in two clusters respectively in the top right and bottom left parts of the periodic table. This is also consistent with intuition, since ionic compounds often have large trivial band gaps and elements from these two clusters tend to form ionic compounds. Third, considering group 15 (the pnictogens), we observe that while N, P, and As have negative topogivities (and Sb has a small positive topogivity), Bi has a positive topogivity with a relatively large magnitude. This is consistent with the intuition that Bi often plays a role in topological materials [25]. Finally, we observe a region of high topogivities in the early transition metals – future work could attempt to understand the underlying reasons for this (note that there is a chance that typical oxidation states are artificially inflating these topogivities). Overall, while the element topogivities are parameters whose specific learned values are affected by dataset and modeling limitations (see Supplementary Section S2.F for discussion), the fact that we can extract chemical insights that are consistent with intuition is evidence that a topogivity-based approximate picture can provide a meaningful way to study topological materials.

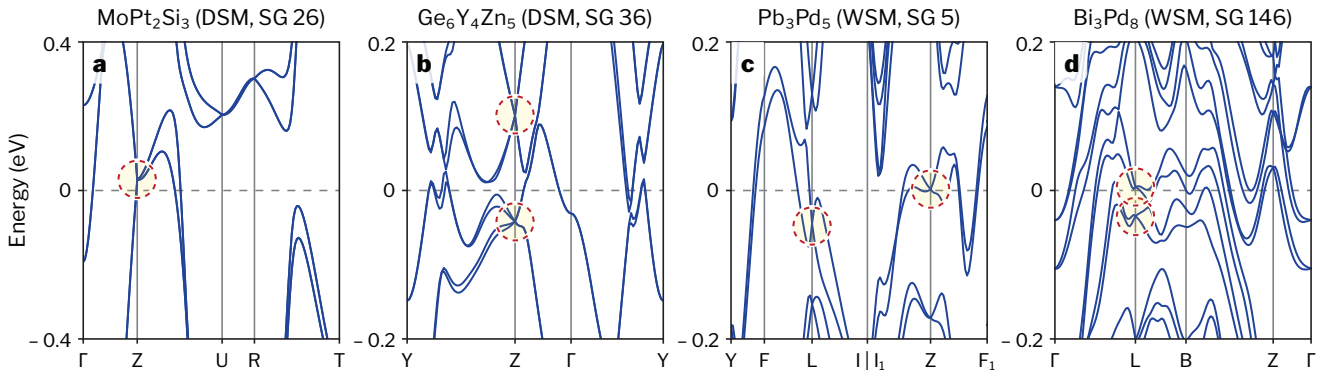


**Figure 3. Selection of newly-discovered topological materials.** These materials are not diagnosable using symmetry indicators [12], but were successfully discovered using our topogivity-based approach. The band structures were computed using DFT.  $\text{MoPt}_2\text{Si}_3$  (a) and  $\text{Ge}_6\text{Y}_4\text{Zn}_5$  (b) are nonsymmorphic Dirac semimetals.  $\text{Pb}_3\text{Pd}_5$  (c) and  $\text{Bi}_3\text{Pd}_8$  (d) are Kramers Weyl semimetals. For each material, relevant topological degeneracies are highlighted by circles.

### HIGH-THROUGHPUT SCREENING AND AB INITIO CALCULATIONS

To identify topological materials using the learned topogivities, we compute  $g(M)$  for each of the 1,433 materials in the discovery space. We restrict our attention to the materials that have a  $g(M)$  value that corresponds to a topologically nontrivial classification with high-confidence (i.e.,  $g(M) \geq 1.0$ ): that leaves 73 materials (after the removal of 2 other materials; see Supplementary Section S3.A). Additionally, since it is difficult to obtain accurate DFT calculations for f-electron materials, we exclude any material that contains a 4f or 5f electron, eliminating 5 materials and thus leaving us with 68 materials for ab initio validation.

For each of these 68 materials, we perform DFT within the generalized gradient approximation (GGA) [42]. We include spin-orbital coupling in all of our calculations, which is consistent with the database [17] (note that topological classification can depend on the presence or absence of spin-orbital coupling [12]). In our DFT calculations, we checked for many – but not all – types of topological materials. In principle it is possible that some topological materials were not detected by our DFT. Further methodological details are provided in Supplementary Section S3.B.

Of the 68 materials, we find 56 topological materials, corresponding to a success rate of 82.4%. The topological materials consist of 48 Weyl semimetals, 7 Dirac semimetals, and 1 Dirac nodal line semimetal (Supplementary Section S4). We note that there are aspects of our procedure and data analysis that could have introduced some bias into the success rate (see Supplementary Section S3.C). Some of these 56 topological materials have previously been predicted in the literature and a smaller portion have also already been experimentally observed, e.g., TaAs [7]. More importantly, our DFT calculations also identify multiple new topological materials that to our knowledge have not been previously identified.

The band structures of four particularly interesting newly-discovered topological materials are shown in Fig. 3. Each is a topological semimetal with a relatively clean band structure

and at least one band crossing within 50 meV of the Fermi level, making it promising for potential experimental investigation.  $\text{MoPt}_2\text{Si}_3$  and  $\text{Ge}_6\text{Y}_4\text{Zn}_5$  are both nonsymmorphic Dirac semimetals. At the Z point, the former has a Dirac point in the valence band manifold and the latter has Dirac points in both the valence and conduction band manifolds.  $\text{Pb}_3\text{Pd}_5$  and  $\text{Bi}_3\text{Pd}_8$  are both Kramers Weyl semimetals [43]. The former has Weyl nodes at the L and Z points, and the latter has two Weyl nodes close in energy at the L point. In particular, we highlight that  $\text{MoPt}_2\text{Si}_3$  has a Dirac point close to the Fermi level as well as a relatively clean Fermi surface, and  $\text{Pb}_3\text{Pd}_5$  has a Weyl node located at the Z point that is right at the Fermi level. We emphasize that the reason the band degeneracies in these four materials are non-symmetry-diagnosable is that they are all within the valence band manifold or conduction band manifold. Such band degeneracies cannot be diagnosed by the symmetry indicators method, which is formulated based on the electron filling and therefore cannot target band degeneracies that are not *between* the valence and conduction bands [12]. The band structures of all of the topogivity-identified topological materials are included in the Supplementary Material.

### DISCUSSION AND OUTLOOK

It is important to note that topogivity is not an unambiguously defined quantity, as its exact numerical value for each element can depend, for example, on the choice of machine learning algorithm and the use of the weighted average formulation (Supplementary Section S2.F). Moreover, the topogivity approach provides only a coarse-grained topological classification – nontrivial or trivial – without the fine-grained detail of ab initio approaches.

Nevertheless, topogivity offers a broadly applicable and simple approach for diagnosing topological materials. This diagnosis uses only the chemical formula and requires merely a handful of arithmetic operations to evaluate. Furthermore, the periodic table of topogivities (Fig. 2) provides simple intuition for a complex, exotic phenomenon. An important highlight of the topogivity approach is that it enables the discovery of

non-symmetry-diagnosable topological materials.

One worthy future direction is to look for a more complete understanding of the underlying reasons for the values of the elements' topogivities, which may in turn shed new light on the fundamental question of why some materials are topological while others are not. Another promising path forward would be to perform more comprehensive searches for new topological materials using topogivity-based strategies. Finally, it is intriguing to contemplate whether our interpretable-ML approach, used here to discover topogivity, could perhaps be used for other material properties as well, such as ferroelectricity, ferromagnetism, or maybe even superconductivity.

### ACKNOWLEDGEMENTS

We thank Pawan Goyal for assisting preliminary work. We thank Samuel Kim, Peter Lu, Rumen Dangovski, and Edward Zhang for helpful discussions. We thank Feng Tang and Xiang-gang Wan for the sharing of materials data. We thank Paola Rebusco for critical reading and editing of the manuscript. A.M. acknowledges support from the MIT EECS Alan L. McWhorter Fellowship and from the National Science Foundation Graduate Research Fellowship under Grant No. 1745302. Research was sponsored in part by the United States Air Force Research Laboratory and the United States Air Force Artificial Intelligence Accelerator and was accomplished under Cooperative Agreement Number FA8750-19-2-1000. The views and conclusions contained in this document are those of the authors

and should not be interpreted as representing the official policies, either expressed or implied, of the United States Air Force or the U.S. Government. The U.S. Government is authorized to reproduce and distribute reprints for Government purposes notwithstanding any copyright notation herein. This material is also based upon work supported in part by the Air Force Office of Scientific Research under the awards number FA9550-20-1-0115, FA9550-21-1-0299, and FA9550-21-1-0317, as well as in part by the US Office of Naval Research (ONR) Multidisciplinary University Research Initiative (MURI) grant N00014-20-1-2325 on Robust Photonic Materials with High-Order Topological Protection. This material is also based upon work supported in part by the U. S. Army Research Office through the Institute for Soldier Nanotechnologies at MIT, under Collaborative Agreement Number W911NF-18-2-0048. This work is also supported in part by the the National Science Foundation under Cooperative Agreement PHY-2019786 (The NSF AI Institute for Artificial Intelligence and Fundamental Interactions, <http://iaifi.org/>). The work of Y.Z. and L.F. was supported by DOE Office of Basic Energy Sciences, Division of Materials Sciences and Engineering under Award DE-SC0018945 (theoretical analysis) and DE-SC0019275 (band structure calculation). L.F. was partly supported by the Simons Investigator Award from Simons Foundation. The work of H.C.P. was partly supported by a Pappalardo Fellowship at MIT.

### CODE AND DATA AVAILABILITY

The code and data underlying our machine learning model will be made available in a public repository.

- 
- [1] L. Fu, C. L. Kane, and E. J. Mele, *Phys. Rev. Lett.* **98**, 106803 (2007).
- [2] D. Hsieh, D. Qian, L. Wray, Y. Xia, Y. S. Hor, R. J. Cava, and M. Z. Hasan, *Nature* **452**, 970 (2008).
- [3] L. Fu, *Phys. Rev. Lett.* **106**, 106802 (2011).
- [4] T. H. Hsieh, H. Lin, J. Liu, W. Duan, A. Bansil, and L. Fu, *Nat. Commun.* **3**, 1 (2012).
- [5] W. A. Benalcazar, B. A. Bernevig, and T. L. Hughes, *Science* **357**, 61 (2017).
- [6] Z. Liu, B. Zhou, Y. Zhang, Z. Wang, H. Weng, D. Prabhakaran, S.-K. Mo, Z. Shen, Z. Fang, X. Dai, *et al.*, *Science* **343**, 864 (2014).
- [7] S.-Y. Xu, I. Belopolski, N. Alidoust, M. Neupane, G. Bian, C. Zhang, R. Sankar, G. Chang, Z. Yuan, C.-C. Lee, *et al.*, *Science* **349**, 613 (2015).
- [8] A. Burkov, M. Hook, and L. Balents, *Phys. Rev. B* **84**, 235126 (2011).
- [9] B. Bradlyn, J. Cano, Z. Wang, M. Vergniory, C. Felser, R. J. Cava, and B. A. Bernevig, *Science* **353**, 558 (2016).
- [10] J. Xiao and B. Yan, *Nat. Rev. Phys.* **3**, 283 (2021).
- [11] A. Bansil, H. Lin, and T. Das, *Rev. Mod. Phys.* **88**, 021004 (2016).
- [12] H. C. Po, A. Vishwanath, and H. Watanabe, *Nat. Commun.* **8**, 1 (2017).
- [13] B. Bradlyn, L. Elcoro, J. Cano, M. Vergniory, Z. Wang, C. Felser, M. Aroyo, and B. A. Bernevig, *Nature* **547**, 298 (2017).
- [14] L. Fu and C. L. Kane, *Phys. Rev. B* **76**, 045302 (2007).
- [15] J. Kruthoff, J. de Boer, J. van Wezel, C. L. Kane, and R.-J. Slager, *Phys. Rev. X* **7**, 041069 (2017).
- [16] Z. Song, T. Zhang, Z. Fang, and C. Fang, *Nat. Commun.* **9**, 1 (2018).
- [17] F. Tang, H. C. Po, A. Vishwanath, and X. Wan, *Nature* **566**, 486 (2019).
- [18] T. Zhang, Y. Jiang, Z. Song, H. Huang, Y. He, Z. Fang, H. Weng, and C. Fang, *Nature* **566**, 475 (2019).
- [19] M. Vergniory, L. Elcoro, C. Felser, N. Regnault, B. A. Bernevig, and Z. Wang, *Nature* **566**, 480 (2019).
- [20] B. Lv, H. Weng, B. Fu, X. P. Wang, H. Miao, J. Ma, P. Richard, X. Huang, L. Zhao, G. Chen, *et al.*, *Phys. Rev. X* **5**, 031013 (2015).
- [21] H. Weng, C. Fang, Z. Fang, B. A. Bernevig, and X. Dai, *Phys. Rev. X* **5**, 011029 (2015).
- [22] W. J. Hehre, *Acc. Chem. Res.* **9**, 399 (1976).
- [23] N. Kumar, S. N. Guin, K. Manna, C. Shekhar, and C. Felser, *Chem. Rev.* **121**, 2780 (2021).
- [24] Q. Gibson, L. M. Schoop, L. Muechler, L. Xie, M. Hirschberger, N. P. Ong, R. Car, and R. J. Cava, *Phys. Rev. B* **91**, 205128 (2015).
- [25] A. Isaeva and M. Ruck, *Inorg. Chem.* **59**, 3437 (2020).
- [26] S. Klemenz, A. K. Hay, S. M. Teicher, A. Topp, J. Cano, and L. M. Schoop, *J. Am. Chem. Soc.* **142**, 6350 (2020).
- [27] X. Gui, I. Pletikosic, H. Cao, H.-J. Tien, X. Xu, R. Zhong, G. Wang, T.-R. Chang, S. Jia, T. Valla, *et al.*, *ACS Cent. Sci.* **5**, 900 (2019).

- [28] M. Zhong, K. Tran, Y. Min, C. Wang, Z. Wang, C.-T. Dinh, P. De Luna, Z. Yu, A. S. Rasouli, P. Brodersen, *et al.*, *Nature* **581**, 178 (2020).
- [29] V. L. Deringer, N. Bernstein, G. Csányi, C. B. Mahmoud, M. Ceriotti, M. Wilson, D. A. Drabold, and S. R. Elliott, *Nature* **589**, 59 (2021).
- [30] J. George and G. Hautier, *Trends Chem.* **3**, 86 (2020).
- [31] Y. Zhang and E.-A. Kim, *Phys. Rev. Lett.* **118**, 216401 (2017).
- [32] P. Zhang, H. Shen, and H. Zhai, *Phys. Rev. Lett.* **120**, 066401 (2018).
- [33] M. S. Scheurer and R.-J. Slager, *Phys. Rev. Lett.* **124**, 226401 (2020).
- [34] Y. Zhang, P. Ginsparg, and E.-A. Kim, *Phys. Rev. Research* **2**, 023283 (2020).
- [35] C. M. Acosta, R. Ouyang, A. Fazzio, M. Scheffler, L. M. Ghiringhelli, and C. Carbogno, *arXiv:1805.10950* (2018).
- [36] N. Claussen, B. A. Bernevig, and N. Regnault, *Phys. Rev. B* **101**, 245117 (2020).
- [37] N. Andrejevic, J. Andrejevic, C. H. Rycroft, and M. Li, *arXiv:2003.00994* (2020).
- [38] G. Cao, R. Ouyang, L. M. Ghiringhelli, M. Scheffler, H. Liu, C. Carbogno, and Z. Zhang, *Phys. Rev. Mater.* **4**, 034204 (2020).
- [39] H. Liu, G. Cao, Z. Zhou, and J. Liu, *J. Phys.: Condens. Matter* **33**, 325501 (2020).
- [40] G. R. Schleder, B. Focassio, and A. Fazzio, *Appl. Phys. Rev.* **8**, 031409 (2021).
- [41] M. G. Vergniory, B. J. Wieder, L. Elcoro, S. S. Parkin, C. Felser, B. A. Bernevig, and N. Regnault, *arXiv:2105.09954* (2021).
- [42] J. P. Perdew, K. Burke, and M. Ernzerhof, *Phys. Rev. Lett.* **77**, 3865 (1996).
- [43] G. Chang, B. J. Wieder, F. Schindler, D. S. Sanchez, I. Belopolski, S.-M. Huang, B. Singh, D. Wu, T.-R. Chang, T. Neupert, *et al.*, *Nat. Mater.* **17**, 978 (2018).